

Evidence for QGP in Pb–Pb 158 A GeV collisions from strange particle abundances and the Coulomb effect

Jean Letessier and Johann Rafelski

Laboratoire de Physique Théorique et Hautes Energies
Université Paris 7, 2 place Jussieu, F-75251 Cedex 05.
Department of Physics, University of Arizona, Tucson, AZ 85721

June 24, 1998

Abstract

The hadronic particle production data from relativistic nuclear Pb–Pb 158 A GeV collisions are successfully described within the chemical non-equilibrium model, provided that the analysis does not include Ω and $\bar{\Omega}$ abundances. We show that there is a subtle influence of the Coulomb potential on strange quarks in quark matter which is also seen in our data analysis, and this Coulomb effect confirms the finding made in the S–Au/W/Pb 200 A GeV collisions that the hadron source is deconfined with respect to strange quark propagation. Physical freeze-out conditions (pressure, specific energy, entropy, and strangeness) are evaluated and considerable universality of hadron freeze-out between the two different collision systems is established.

Intense experimental and theoretical work proceeds to explore the mechanisms of quark confinement effect and the properties of the vacuum state of quantum-chromodynamics (QCD), the non-Abelian gauge theory of ‘color’ charges [1]. Relativistic energy nuclear collisions are the novel experimental tool developed in the past decade to form, study, and explore the ‘melted’ space-time domain, where we hope to find, beyond the critical Hagedorn temperature $T_c \simeq 160$ MeV [2], freely propagating quarks and gluons in the (color charge) plasma (QGP). There is little doubt that this was in the early Universe the transient state of matter, and that only about 20–40 μ sec into evolution did our present confining vacuum freeze-out from the primordial QGP-form. The issue is, if in the attempt to recreate this stage of the evolution of the Universe in laboratory experiments, we can indeed form and study the primordial QGP phase. In some aspects, such as specific entropy and baryon content, notable differences of the laboratory QGP state from the early Universe conditions are expected to arise, not to mention the short laboratory lifespan $\tau_q \simeq 0.5 \cdot 10^{-22}$ sec.

There is also the difficult problem of proving the fundamental paradigm beyond a shade of doubt [3]: is there indeed locally deconfined state formed with energy density exceeding by an order of magnitude that of nuclear matter? Much of the current effort is devoted to this challenge. Among several proposed approaches to study of deconfinement, our work relies on the idea of strangeness flavor enhancement, and the associated enhancement of (strange) antibaryon formation [4, 5, 6]. While both these effects have been confirmed experimentally [7], it is here and now that we believe to draw a definitive conclusion, given the advances of experimental and theoretical methods. We address here 15 particle yield ratios obtained in central Pb–Pb 158 A GeV collision experiments carried out at CERN-SPS. However, four data points involve Ω and $\bar{\Omega}$ particles and even a cursory study of the abundance data shows that these entirely strange particles are not falling into the same systematic class, a fact already seen in their unusual spectral slopes [8]. We believe in view of the difference in systematics that it is appropriate also to consider the data excluding the Ω and $\bar{\Omega}$ yields from analysis. In that case our analysis contains 11 relative experimental particle yields. As we shall discuss, there are up to 5 parameters in our description. In the different analysis discussed here we thus have no less than 6 degrees of freedom (dof). Since we address ratios of strange particles as well as ratios of total

abundances of positive and negative hadrons, we combine in present analysis strangeness observables with the entropy enhancement [9]. While it is quite obvious that color deconfined state is, in general more entropy rich, since the color bonds are broken, the mechanism responsible for entropy production and thermalization, and thus loss of reversibility (decoherence) on the sub-nuclear scale is not understood.

Underlying our data analysis is thus the assumption of local thermal (*i.e.*, energy equipartition) equilibrium. Aside of the thermal appearance of produced particle spectra [2, 10, 11], also the qualitative and systematic agreement over many orders of magnitude between properties of a thermal hadron system and the experimental particle abundance data provides a solid foundation for the assumption of thermal equilibrium [12]. However, in our approach there is a key refinement not present in earlier work: we do not assume chemical equilibrium even for light quarks [13]. Consideration of non-equilibrium chemical abundance for strange quarks allowed to analyze accurately the experimental particle abundance data [14, 15, 16, 17], and to characterize precisely the properties of the presumably deconfined source [11]. The mechanisms of chemical equilibration requiring reactions which change particle abundances are today much better understood theoretically than those responsible for what is believed to be much faster thermal (kinetic) equilibration, where momentum exchange between existent particles is the key mechanism.

Hadronic particles we observe are either emitted directly or are descendants of other hadronic primaries produced near or at surface of the dense matter fireball. Local rest-frame temperature T and local collective flow velocity \vec{v}_c characterize the momentum space distribution of particles emerging from the surface region of the fireball. In addition, each surface volume element is characterized by chemical abundance factors we shall discuss in more detail below. Only particles of similar mass and cross section experience similar drag forces arising from local flow of matter and hence ratio of their abundances in some limited region of phase space for not too small momenta is expected to remain unaltered by \vec{v}_c . Since the surface vector flow \vec{v}_c is a priori largely unknown, in order to use limited ‘windows’ of particle momenta (rapidity y and transverse mass m_\perp) for determination of chemical freeze-out properties of the source, only ratios of ‘mutually compatible’ particles can be considered, aside of ratios of total particle abundances.

The thermal production yield dN_i of particles emitted within the time dt from a locally at rest surface element dS is:

$$dN_i = \frac{dS d^3 p}{(2\pi)^3} A_i v_i dt. \quad (1)$$

Here $v_i = dz/dt$ is the particle velocity normal to the surface element $dS = dx dy$. For a thermal quark-gluon gas source and allowing for recombination-fragmentation of constituents and detailed balance, the complete phase space occupancy factor A_i is given by:

$$A_i = g_i \lambda_i \gamma_i e^{-E_i/T}, \quad \lambda_i = \prod_{j \in i} \lambda_j, \quad \gamma_i = \prod_{j \in i} \gamma_j, \quad E_i = \sum_{j \in i} E_j, \quad (2)$$

where g_i is the degeneracy of the produced particle, and E_i its energy. The valance quark content $\{j\}$ in hadron $\{i\}$ is implied in Eq. (2). The fugacities λ_j arise from conservation laws, in our context, of quark (baryon) number and strangeness in the particle source. $\lambda_q \equiv e^{\mu_q/T}$ is thus the fugacity of the valance light quarks. For a nucleon $\lambda_N = \lambda_q^3$, and hence the baryochemical potential is: $\mu_b = 3\mu_q$. Similarly, for strange quarks we have $\lambda_s \equiv e^{\mu_s/T}$. For an antiparticle fugacity $\lambda_{\bar{s}} = \lambda_s^{-1}$. Some papers refer in this context to hyper-charge fugacity $\lambda_S = \lambda_q/\lambda_s$, thus $\mu_S = \mu_q - \mu_s$. This is a highly inconvenient historical definition arising from considerations of a hypothetical hadron gas phase. It hides from view important symmetries, such as $\lambda_s \rightarrow 1$ for a state in which the phase space size for strange and anti-strange quarks is the same: at finite baryon density the number of hyperons is always greater than the number of anti-hyperons and thus the requirement $\langle N_s - N_{\bar{s}} \rangle = 0$ can only be satisfied for some nontrivial $\lambda_s(\lambda_q) \neq 1$. Thus even a small deviation from $\lambda_s \rightarrow 1$ limit must be fully understood in order to argue that the source is deconfined. Conversely, observation of $\lambda_s \simeq 1$ consistently at different experimental conditions is a strong and convincing argument that at least the strange quarks are unbound, *i.e.*, deconfined.

As this discussion also illustrates, the parameter λ_s does not regulate the total number of $s-\bar{s}$ quark-pairs present in the system. More generally, any compound object comprising a particle-antiparticle pair is not controlled in abundance by a fugacity, since the formation of such particles does not impact the conservation

laws. In consequence, the abundance of, *e.g.*, neutral pions comprises no quark fugacity. This is the reason to introduce an additional chemical phase space occupancy factor γ_i : the effective fugacity of quarks is $\lambda_i \gamma_i$ and antiquarks $\lambda_i^{-1} \gamma_i$. This parameter allows to control pair abundance independently of other properties of the system, and in particular temperature. For $\gamma_i \rightarrow 1$ one reaches a entropy maximum [18], corresponding to the ‘absolute’ chemical equilibrium [6]. Therefore the factor γ_i is called the (chemical) phase space occupancy factor.

A time dependent build up of chemical abundance was first considered in the context of microscopic strangeness production in QGP [5, 19], after it was realized that strange flavor production occurs at the same time scale as the collision process. More generally, one must expect, considering the time scales, that all quark flavors will not be able to exactly follow the rapid evolution in time of dense hadronic matter. Moreover, fragmentation of gluons in hadronizing QGP can contribute additional quark pair abundance, conveniently described by the factor γ_i . It is thus to be expected that also for light quarks the chemical phase space occupancy factor $\gamma_q \neq 1$. Introduction of the factor γ_q leads to a precise chemical description of the S–Au/W/Pb 200 A GeV collisions [13], which was not possible before. The tacit choice $\gamma_q = 1$ has not allowed previously to distinguish the different reaction scenarios in Pb–Pb collisions [16], where we found analyzing the experimental data that hadronic particles could be born either at high temperature $T \simeq 300$ MeV or at expected hadronization temperature $T \simeq 150$ MeV. Introduction of γ_q , along with improvement in precision, and a greater data sample, allowed us to recognize the systematic difference between data points containing, and resp., not containing Ω , $\bar{\Omega}$, allowing us to develop the precise analysis here presented.

In another refinement both u , d -flavor fugacities λ_u and λ_d can be introduced, allowing for up-down-quark asymmetry [20]. We recall that by definition $2\mu_q = \mu_d + \mu_u$, thus $\lambda_q \equiv \sqrt{\lambda_u \lambda_d}$. For the highly Coulomb-charged fireballs formed in Pb–Pb collisions a further effect of the same relative magnitude which needs consideration is the distortion of the particle phase space by the Coulomb potential. This effect influences particles and antiparticles in opposite way, and has by factor two different strength for u -quark (charge $+2/3|e|$) and (d, s) -quarks (charge $-1/3|e|$). Because Coulomb-effect acts in opposite way on u and d quarks, its net impact on λ_q is relatively small as we shall see.

However, the Coulomb effect distorts significantly the expectation regarding $\lambda_s \rightarrow 1$ for strangeness-deconfined source with vanishing net strangeness. The difference between strange and anti-strange quark numbers (net strangeness) allowing for a Coulomb potential within a relativistic Thomas-Fermi phase space occupancy model [21], allowing for finite temperature in QGP is:

$$\langle N_s - N_{\bar{s}} \rangle = \int_{R_f} g_s \frac{d^3 r d^3 p}{(2\pi)^3} \left[\frac{1}{1 + \gamma_s^{-1} \lambda_s^{-1} e^{(E(p) - \frac{1}{3}V(r))/T}} - \frac{1}{1 + \gamma_s^{-1} \lambda_s e^{(E(p) + \frac{1}{3}V(r))/T}} \right], \quad (3)$$

which clearly cannot vanish for $V \neq 0$ in the limit $\lambda_s \rightarrow 0$. In Eq. (3) the subscript on the spatial integral reminds us that only the classically allowed region within the fireball is covered in the integration over the level density; $E = \sqrt{m^2 + \vec{p}^2}$, and for a uniform charge distribution within a radius R_f of charge Z_f :

$$V = \begin{cases} -\frac{3}{2} \frac{Z_f e^2}{R_f} \left[1 - \frac{1}{3} \left(\frac{r}{R_f} \right)^2 \right], & \text{for } r > R_f; \\ -\frac{Z_f e^2}{r}, & \text{for } r > R_f. \end{cases} \quad (4)$$

One obtains a rather precise result for the range of parameters of interest to us (see below) using the Boltzmann approximation:

$$\langle N_s - N_{\bar{s}} \rangle = \gamma_s \left\{ \int g_s \frac{d^3 p}{(2\pi)^3} e^{-E/T} \right\} \int_{R_f} d^3 r \left[\lambda_s e^{\frac{V}{3T}} - \lambda_s^{-1} e^{-\frac{V}{3T}} \right]. \quad (5)$$

The Boltzmann limit allows also to verify the signs: the Coulomb potential is negative for the negatively charged s -quarks with the magnitude of the charge, $1/3$, made explicit in the potential terms in all expressions above. It turns out that there is always only one solution, with resulting $\lambda_s > 1$. The magnitude of the effect is quite significant: choosing $R_f = 8$ fm, $T = 140$ MeV, $m_s = 200$ MeV (value of $0.5 < \gamma_s < 2$ is irrelevant)

solution of Eq. (3) for $Z_f = 150$ yields $\lambda_s = 1.10$ (precisely: 1.0983, 1.10 corresponds to $R_f = 7.87$ fm). This result is consistent with one of the scenarios we reported in [16] for Pb–Pb collisions. Thus we are reassured that the experimental data is very likely consistent with deconfined quark source, and hence a detailed verification of this hypothesis is needed. The remarkable result we shall find below fitting experimental data is indeed this value $\lambda_s = 1.10 \pm 0.02$, see table 1. Thus as before for the lighter system S-Au/W/Pb [13, 14, 20] we are finding that the source of strange hadrons (up to Coulomb-asymmetry) is governed by a symmetric, and thus presumably deconfined strange quark phase space.

To better understand the situation it is convenient to introduce a charge conservation fugacity λ_Q . The abundance of charged quarks is thus counted by the fugacities:

$$\lambda_s \equiv \tilde{\lambda}_s \lambda_Q^{-1/3}, \quad \lambda_d \equiv \tilde{\lambda}_d \lambda_Q^{-1/3}, \quad \lambda_u \equiv \tilde{\lambda}_u \lambda_Q^{2/3}, \quad \lambda_q = \sqrt{\lambda_u \lambda_d} \equiv \tilde{\lambda}_q \lambda_Q^{1/6}. \quad (6)$$

Given that quark flavor is conserved, and thus charge is conserved implicitly too, λ_Q is not another independent statistical variable, it is determined by the Coulomb potential:

$$\lambda_Q \equiv \frac{\int d^3r e^{\frac{V}{T}}}{\int d^3r}. \quad (7)$$

The difference between λ_q and $\tilde{\lambda}_q$, see Eq. (6) is at the level of 1–2% considering the Pb–Pb case, and yet smaller for S–A reactions. However, the individual light quark fugacities experience more significant shifts as we saw for λ_s . We note that all previous studies of QGP state properties referred to the tilde-fugacities, while all data analysis where obtained for the non-tilde fugacities. Even though charge conservation has been enforced previously [17], this was done without allowance for the Coulomb deformation of the phase space and hence there was no net difference between tilde and non-tilde quantities for large systems (small systems experience the effect of exact canonical quantum number conservation [22]). We conclude that a QGP source in order to conserved strangeness has indeed $\tilde{\lambda}_s = 1$, which implies $\lambda_s = \lambda_Q^{-1/3}$ in the fitted hadron distributions, and moreover [14]:

$$\frac{\langle d - \bar{d} \rangle}{\langle u - \bar{u} \rangle} = \frac{2A - Z}{A + Z} = \frac{\tilde{\mu}_d}{\tilde{\mu}_u} = \frac{\ln \tilde{\lambda}_d}{\ln \tilde{\lambda}_u}. \quad (8)$$

For Pb–Pb collisions with $A = 208$ and $Z = 82$ there is indeed a non-negligible isospin asymmetry, but the Coulomb effect slightly over-compensates it and hence $\mu_u > \mu_d$, while $\tilde{\mu}_u < \tilde{\mu}_d$.

Let us briefly explain how we obtain the statistical parameters of the fits shown in table 1: with $E_i = \sqrt{m_i^2 + p^2} = \sqrt{m_i^2 + p_\perp^2} \cosh y$ we integrate over the transverse momentum range as given by the experiment, see table 2. To obtain the relative strengths of centrally produced particles we consider only central rapidity region $y \simeq 0$. We allow all hadronic resonances to disintegrate in order to obtain the final relative multiplicity of ‘stable’ particles required to form the observed particle ratios. We show results of four main fits denoted A, B, C, D in top section of table 1, fitting data described in first 4 columns of table 2. In this group of fits to experimental results we successively relax the chemical variables from their tacit values ($= 1$). In each step the number of degrees of freedom in the fit decreases by one, yet the fit becomes, as described by χ^2/dof progressively better, and is indeed of amazingly impressive quality, with $\chi^2/\text{dof} = 0.27$ when all 4 chemical variables are free in the data fit. We thus conclude that it is necessary in description of the particle abundance data to allow non-equilibrium abundances of light and strange quarks.

It is very clearly seen in the bottom section of table 2 that the results comprising Ω and $\bar{\Omega}$ -particles do not follow the same systematics, a fact already reported with respect of their spectral temperature by the WA97 collaboration [8]. A possible hypothesis is that a good fraction of these particles are made in processes that are different in nature than those leading to the other particle abundances, and hence we excluded Ω and $\bar{\Omega}$ -particles from all but one of the data fits, denoted F. Moreover, if some strange particles hadronize separately, on cannot demand that the remaining particles balance strangeness exactly and hence we did not in general enforce in the fit strangeness conservation, except in fit D_s. That this fit is only slightly worse than fit D implies that the source for both Ω and $\bar{\Omega}$ is nearly symmetric with respect to abundance of strange and anti-strange quarks. This is consistent with the observation that much of the significant asymmetry in the

Table 1: Statistical parameters obtained from fits to experimental results shown in table 2. Values of λ_s in fit D_s is the result of strangeness conservation constraint (not fitted): asterisk * means a fixed (input) value, not a parameter of fit. In fit D_t the temperature is fixed at the value obtained for S–Au/W/Pb collisions, and in fit D_p , the pressure in the hadronic phase space is fitted to 82 ± 6 MeV/fm 3 , also the value obtained in S–Au/W/Pb collisions. In fit F the four ratios with Ω -data are also fitted.

Fit	T_f [MeV]	λ_q	λ_s	γ_s	γ_q	χ^2/dof
A	147 ± 3	1.69 ± 0.03	1^*	1^*	1^*	14
B	142 ± 3	1.70 ± 0.03	1.10 ± 0.02	1^*	1^*	11
C	144 ± 4	1.62 ± 0.03	1.10 ± 0.02	0.63 ± 0.04	1^*	3.4
D	134 ± 3	1.62 ± 0.03	1.10 ± 0.02	1.27 ± 0.08	1.84 ± 0.30	0.27
D_s	133 ± 3	1.63 ± 0.03	$1.09^* \pm 0.02$	1.98 ± 0.12	2.75 ± 0.35	0.38
D_t	143^*	1.61 ± 0.03	1.10 ± 0.02	0.74 ± 0.06	1.15 ± 0.18	0.65
D_p	137 ± 4	1.62 ± 0.03	1.10 ± 0.02	0.88 ± 0.07	1.33 ± 0.10	0.45
F	334 ± 18	1.61 ± 0.03	1.12 ± 0.02	0.09 ± 0.01	0.18 ± 0.02	1.94

Table 2: Particle ratios: Experimental results for Pb–Pb, references and kinematic domain in first four columns, and different fits corresponding to those shown in table 1 in the remaining columns; Asterisk * means the corresponding experimental result is not fitted.

Ratios	Ref.	cuts[GeV]	Exp. data	Fit A	Fit B	Fit C	Fit D	Fit D_s	Fit D_t	Fit D_p	Fit F
Ξ/Λ	1	$p_\perp > 0.7$	0.099 ± 0.008	0.130	0.138	0.093	0.095	0.098	0.095	0.093	0.107
$\bar{\Xi}/\bar{\Lambda}$	1	$p_\perp > 0.7$	0.203 ± 0.024	0.361	0.322	0.198	0.206	0.215	0.201	0.201	0.216
$\bar{\Lambda}/\Lambda$	1	$p_\perp > 0.7$	0.124 ± 0.013	0.126	0.100	0.121	0.120	0.119	0.123	0.120	0.121
Ξ/Ξ	1	$p_\perp > 0.7$	0.255 ± 0.025	0.351	0.232	0.258	0.260	0.263	0.262	0.258	0.246
$\frac{(\Xi+\bar{\Xi})}{(\Lambda+\bar{\Lambda})}$	2	$p_\perp > 1.$	0.13 ± 0.03	0.169	0.169	0.114	0.118	0.122	0.116	0.115	0.120
K_s^0/ϕ	3,4		11.9 ± 1.5	6.42	6.3	10.4	9.89	9.69	10.1	10.2	16.1
K^+/K^-	5		1.80 ± 0.10	2.27	1.96	1.75	1.76	1.73	1.73	1.77	1.62
p/\bar{p}	6		$18.1 \pm 4.$	20.5	22.0	17.1	17.3	17.9	16.6	17.3	16.7
Λ/\bar{p}	7		$3. \pm 1.$	2.97	3.02	2.91	2.68	3.45	2.91	2.96	0.65
K_s^0/B	3		0.183 ± 0.027	0.298	0.305	0.224	0.194	0.167	0.211	0.214	0.242
h^-/B	3		1.83 ± 0.2	1.30	1.47	1.59	1.80	1.86	1.55	1.72	1.27
Ω/Ξ	1	$p_\perp > 0.7$	0.192 ± 0.024	0.115*	0.119*	0.080*	0.078*	0.080*	0.082*	0.078*	0.192
$\bar{\Omega}/\bar{\Xi}$	8	$p_\perp > 0.7$	0.27 ± 0.06	0.32*	0.28*	0.17*	0.17*	0.18*	0.18*	0.17*	0.40
$\bar{\Omega}/\Omega$	1	$p_\perp > 0.7$	0.38 ± 0.10	1.00*	0.55*	0.56*	0.57*	0.59*	0.56*	0.56*	0.51
$\frac{(\Omega+\bar{\Omega})}{(\Xi+\bar{\Xi})}$	8	$p_\perp > 0.7$	0.20 ± 0.03	0.17*	0.15*	0.10*	0.10*	0.10*	0.10*	0.10*	0.23

¹ I. Králik, for the WA97 Collaboration, *Nucl. Phys. A* (1998) (proceedings of Tsukuba QM1998 meeting).

² G.J. Odyniec, for the NA49 Collaboration, *J. Phys. G* **23**, 1827 (1997).

³ P.G. Jones, for the NA49 Collaboration, *Nucl. Phys. A* **610**, 188c (1996).

⁴ F. Pühlhofer, for the NA49 Collaboration, *Nucl. Phys. A* (1998) (proceedings of Tsukuba QM1998 meeting).

⁵ C. Bormann, for the NA49 Collaboration, *J. Phys. G* **23**, 1817 (1997).

⁶ G.J. Odyniec, *Nucl. Phys. A* (1998) (proceedings of Tsukuba QM1998 meeting).

⁷ D. Röhrlig, for the NA49 Collaboration, “Recent results from NA49 experiment on Pb–Pb collisions at 158 GeV per nucleon”, see figure 4, in proceedings of EPS-HEP Conference, Jerusalem, August 19–26, 1997.

⁸ A.K. Holme, for the WA97 Collaboration, *J. Phys. G* **23**, 1851 (1997).

ratio $\bar{\Omega}/\Omega$ arises from the Coulomb effect we described above. We note that the ‘anomalous’ fit F shown in table 1 performed with the four Ω -particle data points yields $\chi^2/\text{dof}=2$ for 10 dof, the mathematical confidence level of this fit is 3%, it can safely be assumed that our model is not adequately accounting for the production

of Ω -particle as presently reported. It is, however, interesting to note that the production of Ω , $\bar{\Omega}$ demands a rather high temperature, which could be interpreted in terms of early production of these particles by a very hot source. The data is too scarce to pursue this hypothesis further at this time.

The second group of fits in table 1 is obtained implementing physical constraints as indicated by the subscript: D_s includes the requirement of strangeness conservation, i.e. the hadronic phase space has to contain for the given statistical parameters as many \bar{s} - as s -quarks. This is most conveniently accomplished by finding the value of λ_s which balances strangeness in terms of the other fitted parameters, and thus, though not fitted the value shown in table 1 displays an error, derived from the errors determined fitting the other statistical variables. We note that the phase space occupancies change drastically between fits D and D_s , however the value γ_s/γ_q changes from 0.69 for fit D to 0.72 in fit D_s . In actual numerical procedure we took advantage of this stability in γ_s/γ_q -ratio, using it as a parameter. More generally, we note that all acceptable fits shown in table 1 yield $\gamma_s/\gamma_q = 0.68 \pm 0.05$, which is consistent with the result of fit C for γ_s , where the tacit assumption $\gamma_q = 1$ is made.

There is considerable reason to seek a comparison of the Pb–Pb system with the analysis of S–Au/W/Pb reactions which we reported earlier [13]. Thus we consider the fit D_t in which the freeze-out temperature is fixed at the value we found in S–Au/W/Pb reactions, $T_f = 143$ MeV. In fit D_p the pressure of the hadron phase space is chosen at the value we found in S–Au/W/Pb reactions, $P = 82$ MeV/fm³. As judged by χ^2/dof all D_i -fits are possible, and the resulting particle multiplicities presented in the columns of table 2 differ only in minute detail. The two fits D_t and D_p which test consistency with the smaller S–Au/W/Pb reactions are well within the allowable error. This consistency implies the possibility that the matter formed in these two very different systems hadronize in a rather similar fashion, though collective surface flows are very different.

To resolve if there is universal freeze-out we have to consider the physical properties of the fireball. While the statistical parameters shown in table 1 can vary strongly from fit to fit, we find that the implicitly fitted physical properties of the hadron source are more stable. In table 3 we show for the same 8 fits along with their temperature the specific energy and entropy content, and specific anti-strangeness content, along with specific strangeness asymmetry, and finally pressure evaluated by using the fitted statistical parameters to characterize the hadronic particle phase space. We note that it is improper in general to refer to these properties as those of a ‘hadronic gas’ formed in nuclear collisions, as the particles considered may be emitted in sequence, and thus there never is a stage corresponding to a hadron gas phase. However, in the event such a stage exists, we also evaluated (see last column in table 3) the volume of the hadron gas source at chemical decoupling. In order to obtain this extensive property, we used the net baryon number in the fireball being $\langle B - \bar{B} \rangle = 372 \pm 10$ as stated in [17]. Note that a spherical source corresponding to the best fit D would have a source radius 9.6 fm, which in turn can be checked to be exactly in agreement with deconfined strangeness conservation as described by Eq. (3), given the parameters of the fit and $m_s = 200$ MeV. Other interesting conclusions arising in view of these results and shown in table 3 are: the specific energy content E_f/B is well within the expectations based on the collision energy content per nucleon (8.6 GeV) and hence this result confirms firmly the hypothesis that the energy stopping and baryon number stopping in the fireball are very similar. The specific strangeness content of the Pb–Pb collision fireball is, by about 20% smaller than S–Au/W/Pb result.

We now compare the two hadron sources leading to formation of hadronic particles in S–Au/W/Pb, and in Pb–Pb collision fireballs (*cf.* table 3 and [13]). This comparison yields a surprise shown in Fig. (1): we see here as function of given freeze-out temperature, with other parameters determined by least square fit to the experimental results, that all the different physical properties of the hadronic source agree for the both collision systems, solid lines are for Pb–Pb and dashed lines are for the lighter S–Au/W/Pb fireballs. There is a common hadronization point in all curves arising near $T_f = 143$ MeV, the best value in the S–Au/W/Pb system [13], and for this reason we have provided above the results for the related fit D_t . These results, along with earlier shown strange phase space symmetry and the Coulomb effect has as simple interpretation the formation of a deconfined phase in the initial stages of the collision, which subsequently evolves and flows apart till it reaches the universal hadronization point, with many similar physical properties, independent of the collision system. System dependent will certainly be the surface collective velocity \vec{v}_c , however, our analysis was organized such that this vector field did not enter.

In conclusion, we have presented detailed analysis of hadron abundances observed in central Pb–Pb in-

Table 3: Physical properties of hadronic final state phase space (specific energy, entropy, anti-strangeness, net strangeness, pressure and volume) derived from fits of Pb–Pb data in table 2. Asterisk * means fixed input.

Fit	T_f [MeV]	E_f/B	S_f/B	\bar{s}_f/B	$(\bar{s}_f - s_f)/B$	P_f [GeV/fm 3]	V_f [fm 3]
A	147 ± 3	6.60 ± 0.40	37.0 ± 3	0.92 ± 0.05	0.29 ± 0.02	0.068 ± 0.005	6429 ± 500
B	142 ± 3	7.13 ± 0.50	40.9 ± 3	1.02 ± 0.05	0.21 ± 0.02	0.053 ± 0.005	8994 ± 600
C	144 ± 4	7.75 ± 0.50	41.7 ± 3	0.70 ± 0.05	0.14 ± 0.02	0.053 ± 0.005	10242 ± 800
D	134 ± 3	8.33 ± 0.50	46.8 ± 3	0.61 ± 0.04	0.08 ± 0.01	0.185 ± 0.012	3619 ± 250
D_s	133 ± 3	8.72 ± 0.50	48.1 ± 3	0.51 ± 0.04	0^*	0.687 ± 0.030	1134 ± 100
D_t	143^*	7.63 ± 0.45	41.4 ± 3	0.68 ± 0.05	0.12 ± 0.01	0.072 ± 0.005	7517 ± 500
D_p	137 ± 4	8.05 ± 0.50	44.7 ± 3	0.67 ± 0.05	0.13 ± 0.01	0.082^*	7090 ± 500
F	334 ± 18	9.79 ± 0.50	24.1 ± 2	0.78 ± 0.05	0.06 ± 0.01	1.64 ± 0.006	2303 ± 250

teractions at 158 A GeV in terms of thermal equilibrium and chemical non-equilibrium phase space model of (strange) hadronic particles. We assumed formation of a thermal dense matter fireball of unknown structure, which explodes and disintegrates into the final state hadrons. This description has turned out several excellent fits to all abundance data which at present comprise 6 degrees of freedom, yielding a family of fits with highest confidence level. The physical statistical parameters obtained from these fits characterize a strange particle source which, when allowing for Coulomb deformation of the strange and anti-strange quarks is exactly symmetric, as is natural for a deconfined state. While the fitted statistical parameters shown in table 1 can vary widely there is no way to distinguish with naked eye the different fits D, D_s , D_t , D_p inspecting the particle abundances shown in table 2. It is important to take note that along with $\lambda_q = 1.62 \pm 0.03$, $\lambda_s = 1.10 \pm 0.02$ there also is a stable value $\gamma_s/\gamma_q = 0.68 \pm 0.05$. The freeze-out temperature is $130 < T_f < 145$ MeV. Given the statistical parameters we evaluate the physical properties of the hadronic particle phase space, such as energy, entropy and baryon number. The values we find in the final state reflect exactly on the initial state conditions confirming the consistency of the approach and validity of the reaction picture applied. This part of our analysis confirms that the reaction proceeds by the way of the formation of a dense fireball comprising highly excited hadronic matter with the fitted value of λ_s which exactly matches strangeness balance in QGP allowing for the Coulomb effect for particle source of the size $R_f = 9.6 \pm 2$ fm. We compare conditions of the particle source for the two systems Pb–Pb and S–Au/W/Pb and find that both can be seen as hadronizing in same physical conditions.

We return in near future to the question of how the pre-hadron QGP-fireball looks like and what are its detailed statistical and physical properties: we have begun, using quark-gluon plasma equations of state which incorporate the perturbative corrections and thermal masses, to study detailed scenarios of QGP formation and evolution that leads to the freeze-out properties we obtained here. The important preliminary finding is that it is possible to find QGP-fireballs that naturally lead to the results obtained fitting the experimental hadron abundance data, and thus the QGP hypothesis is also consistent with our current theoretical understanding of QGP equations of state[23].

Acknowledgments:

This work was supported in part by a grant from the U.S. Department of Energy, DE-FG03-95ER40937 . LPTHE-Univ. Paris 6 et 7 is: Unité mixte de Recherche du CNRS, UMR7589.

References

- [1] H. Fritzsch, M. Gell-Mann and H. Leutwyler, *Phys. Lett.* **47 B**, 365 (1973);
H.D. Politzer, *Phys. Rep.* **14**, 129-180 (1974) (see p. 154 and Refs. 34-41).
- [2] R. Hagedorn, *Suppl. Nuovo Cimento* **2**, 147 (1965).
R. Hagedorn, Cargèse lectures in Physics, Vol. 6, Gordon and Breach (New York 1977) and references therein.
See also: J. Letessier, H. Gutbrod and J. Rafelski, *Hot Hadronic Matter*, NATO-ASI series B34,6 Plenum Press, New York 1995.
- [3] J. W. Harris and B. Müller, *Ann. Rev. Nucl. Science* **46**, 71 (1996), and references therein; [hep-ph/9602235].
- [4] J. Rafelski, *Phys. Rep.* **88**, 331 (1982); J. Rafelski and R. Hagedorn, in *Statistical Mechanics of Quarks and Hadrons*, p. 253, (North Holland, Amsterdam, 1981); J. Rafelski and M. Danos, *Phys. Lett. B* **192**, 432 (1987).
- [5] J. Rafelski and B. Müller, *Phys. Rev. Lett* **48**, 1066 (1982); **56**, 2334E (1986).
- [6] P. Koch, B. Müller and J. Rafelski, *Phys. Rep.* **142**, 167 (1986).
- [7] G.J. Odyniec, LBL, Berkeley preprint LBL-41336, Jan 1998, to appear in Quark Matter 1997 (Tsukuba) proceedings.
- [8] E. Andersen et al, WA97-collaboration, preprint CERN-EP-98-064, Apr 1998. Submitted to *Phys. Lett. B*.
- [9] J. Rafelski, J. Letessier and A. Tounsi, Dallas-ICHEP (1992) p. 983 (QCD161:H51:1992); [hep-ph/9711350];
J. Letessier, A. Tounsi, U. Heinz, J. Sollfrank and J. Rafelski *Phys. Rev. Lett.* **70**, 3530 (1993); [hep-ph/9711349].
- [10] H. Grote, R. Hagedorn and J. Ranft, *Atlas of Particle Production Spectra*, (CERN-Service d'Information Scientifique, Geneva 1970).
- [11] J. Rafelski, J. Letessier and A. Tounsi, *Acta Phys. Pol. B* **27**, 1035 (1996), and references therein.
- [12] P. Braun-Munzinger, J. Stachel, J.P. Wessels and N. Xu, *Phys. Lett. B* **365**, 1 (1996); [nucl-th/9508020].
- [13] J. Letessier and J. Rafelski, submitted to *Phys. Rev. C*; [hep-ph/9806386].
- [14] J. Rafelski, *Phys. Lett. B* **262**, 333 (1991);
J. Rafelski, *Nucl. Phys. A* **544**, 279c (1992).
- [15] J. Sollfrank, *J. Phys. G* **23**, 1903 (1997); [nucl-th/9707020], and references therein.
- [16] J. Letessier, J. Rafelski and A. Tounsi, *Phys. Lett. B* **410**, (1997) 315; [hep-ph/9710310];
J. Rafelski, J. Letessier, and A. Tounsi, *Acta Phys. Polon.*, **B28**, 2841, (1997); [hep-ph/9710340].
- [17] F. Becattini, M. Gazdzicki and J. Sollfrank, *Eur. Phys. J. C*; (1998) *in press*, [hep-ph/9710529].
- [18] J. Letessier, A. Tounsi and J. Rafelski, *Phys. Rev. C* **50**, 406 (1994); [hep-ph/9711346];
J. Rafelski, J. Letessier and A. Tounsi, *Acta Phys. Pol. A* **85**, 699 (1994).
- [19] T.S. Biro and J. Zimanyi *Phys. Lett. B* **113**, 6 (1982);
T.S. Biro and J. Zimanyi *Nucl. Phys. A* **395**, 525 (1983).
- [20] J. Letessier, A. Tounsi, U. Heinz, J. Sollfrank and J. Rafelski, *Phys. Rev. D* **51**, 3408 (1995).
- [21] B. Muller and J. Rafelski, *Phys. Rev. Lett.* **34**, 349 (1975).
- [22] J. Rafelski and M. Danos, *Phys. Lett. B* **97** 279 (1980).
- [23] J. Letessier and J. Rafelski, "Properties of QGP-fireballs formed in relativistic nuclear collisions at SPS energies", in preparation.

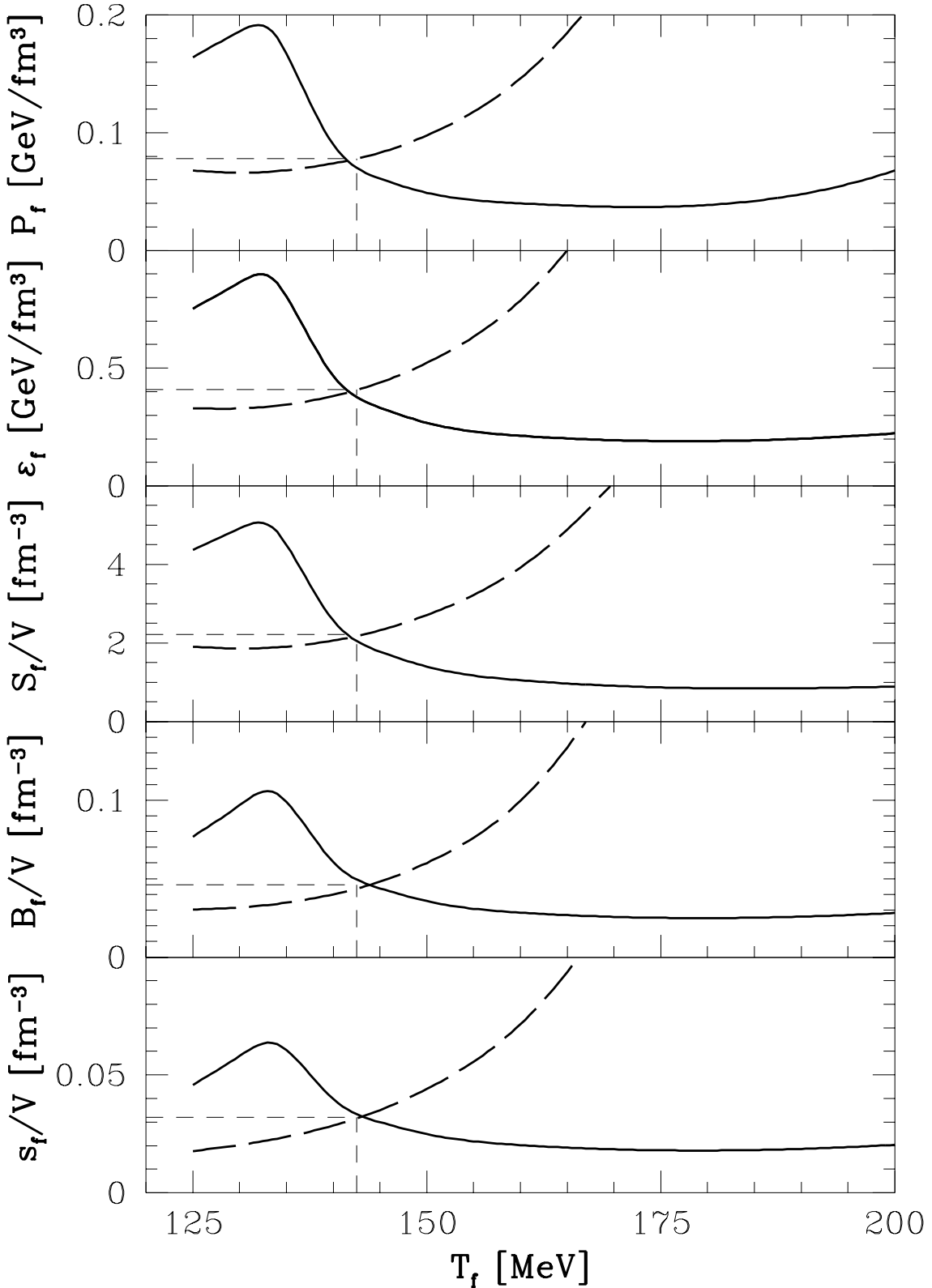


Figure 1: Comparison of the physical properties of the hadron source in Pb–Pb (solid lines) and S–Au/W/Pb (dashed lines) collision fireballs. Curves are results of least square fits to the experimental particle abundance data for given T_f as presented here and in [13]. We show in sequence from top to bottom: pressure P_f , energy density ϵ_f entropy density, S_f/V , baryon density B_f/V and s -quark density s_f/V .